# Smart Grid Simulation Including Communication Network: A Hardware in the Loop Approach

**HARSHAVARDHAN PALAHALLI**[1], **(Member, IEEE), ENRICO RAGAINI**[2], **(Senior Member, IEEE), AND GIAMBATTISTA GRUOSSO**[1], **(Senior Member, IEEE)**

[1]Dipartimento di Elettronica, Informazione e Bioingegneria, Politecnico di Milano, 20133 Milano, Italy
[2]ABB SACE, 24123 Bergamo, Italy

Corresponding author: Giambattista Gruosso (Giambattista.gruosso@polimi.it)

**ABSTRACT** Smart grids are complex electrical systems made up of power devices and communication systems that interact with each other, both locally through measures and generally through the exchange of information on communication networks. In this article, the simulation of a smart grid including the emulation of the communication network behavior together with the physical hardware devices is proposed using hardware-in-the-loop methodology. The original aspect of the technique is related to the fact that the models are generated in a tool that is independent of the real-time simulator using a model-based design approach, and then the code is generated and deployed in a real-time simulator coupled with hardware devices such as low voltage protection units. The proposed framework is used to test the protection coordination that employs the IEC-61850 communication protocol. A test case is shown demonstrating the coordination of switches and the emulation of the PV system in hardware-in-the-loop, focusing on the implementation of the interface algorithm over Ethernet using the UDP communication protocol.

**INDEX TERMS** Co-simulation, hardware-in-the-loop, MATLAB-Simulink, model based design, PV system, protection devices, real-time simulation, smart grid.

## I. INTRODUCTION

The smart grid is a complex system made by power system components, combined with communication network, allowing the distributed control of power grid with the integration of controllers, sensors, and actuators. The use of these kind of grids is the key factor of the coordination of Renewable energy sources. To address the social challenges related to energy, in fact, the coordination of these sources is a strong requirement in the future of power generation combined with storage systems as well the futuristic vision of power exchange between the grid and electric vehicles (EV) [1], [2]. The study of all these scenarios requires to perform rigorous tests before implementation that often cannot be done directly on the power network. The availability of virtual test benches, such as digital twins of the grid, can be an useful aid to perform forecasting and validation of algorithms and devices [3], [4]. The requirements of digital twins must be linked to their ability to interface real physical devices at signal or power level and to simulate the system in real

time. The latter requirement is essential to validate control algorithms or device performance. By utilizing hardware-in-the-loop (HIL) methodology in real-time (RT) simulation, modeled systems can be replaced with the actual physical hardware components [5], [6]. For example, instead of using a simulated controller, a physical controller can be used to control the plant model by exchanging the signals through hardware input-output (IO) channels in real-time. Also, it is possible to feed real-time external data into the emulated system in run-time of the simulation, allowing dynamic measurement of real-world data in simulation instead of infusing data using a pre-written script. The above method is widely used in automobile and aerospace sector [7], [8], [9], but for RT simulation of power system components involving switching devices of power converters require fast processors to reach slower time steps to capture fast transient phenomena [10], [11].

In complex systems like smart grids and other electrical systems, to test the controller, and to integrate actuators and sensors, it is often required to split the mathematical model and need to be emulated in two different hardware [12], [13]. Sometimes it is necessary to do it because of the hardware

The associate editor coordinating the review of this manuscript and approving it for publication was Eyuphan Bulut.

constraints like memory, hardware IO unavailability, etc. Co-simulation is the methodology that is used to emulate the mathematical models in two different platforms and yet running synchronously to deliver results for the same simulation.

Other factors that influence the need for Co-simulation are that the unavailability of a cost-effective computing platform that can deliver all the facility needed for smart grid simulation. There are many platforms available restricting with respect to specific domain, for example, Power system simulators often do not provide network simulators [14], while the converse is also not true. Traditionally, hardware simulators in the loop are hardware and software solutions offered by commercial companies which deliver the advantages of implementation on one hand and on the other hand the limitation of modeling, as it is necessary to use the simulation techniques proposed by them. To study new simulation methodologies, or to implement models already developed in other environments, a great effort of translation is required. Having the ability to use any model and hardware is a strength of the development of digital twins, especially if you think of the need to integrate models provided by different developers of components. Starting from these considerations one of the most original points of this work is to start from models generated in different simulation environments and then transport them in a real-time simulator, by means of code generation. The approach begins with the techniques of Model-Based Design (MBD) [15], [16], and through their ability to generate code, the systems used for our purpose are produced. Especially, cutting edge technology in automatic code generation for platform-specific target hardware helps to transfer created model into the processors without entangling with long scripts and the strict real-time requirements can be implemented writing the solver in a proper way selecting the time step of solvers and the timing scheduling of the operations.

The purpose of this article is twofold, it covers the main aspects of the proposed methodology with two intentions. One is to present the approach in a clear and comprehensive way, and the other is to present an interesting case of a smart grid and simulation that also takes the communication infrastructure into account.

The methodology to conduct a real-time hardware-in-the-loop simulation of the smart grid, using a Co-simulation architecture and physical electric circuit breakers, is firstly presented. The choice is to use non-dedicated hardware to develop the HIL system so as to be able to integrate devices and models described in different languages. The AC section of the microgrid is modeled in model based design (MBD) tool [17], using automatic code generation tool the model is simulated in real-time using Intel's processor of the usual personal computer, or other kind of embedded core that support the real-time extension. The DC section of the microgrid is simulated in another real-time digital simulator based on NI cRIO FPGA hardware [18]. The choice of two different hardware architectures is due to the fact that in the first simulator we consider "slow" behavior of the grid, while in

the second "fast" dynamics such as the switching frequency of the converters are contemplated. To this, the simulation of the communication network is integrated by emulating it in two ways:

1) The first is to connect and synchronously run two power system simulators using an interface via Ethernet over the network, thereby emulating the network behavior.
2) The FPGA in cRIO hardware is also used to drive voltage and current (VI) signals, present in AC section of the microgrid model and applied on ABB's low voltage circuit breakers Emax2 trip units (TU) which are coordinated using IEC 61850 communication protocol.

The proposed method in this article is not the definitive solution for real-time simulation, but it is a good compromise for cheaper and faster design to implementation with the physical hardware and the measuring device integration. In the remaining part of the article the reader can find: section II briefs about related work in Smart grid with its state of the art technology in Co-simulation, section III briefs about Smart grid modeling and different parameters of its components, section IV elaborates the HIL simulation framework proposed in this work, section V shows the test-bench setup used for RT HIL simulation, section VI discusses the obtained results, while the conclusions are drawn in section VII.

## II. RELATED WORKS IN SMART GRID CO-SIMULATION

As the need of integration of many systems of sources and sinks to the smart grid is increasing, design and analysis of these systems are in the mainstream of research, few of them that facades state of the art of Co-simulation technology are presented here. The important considerations while choosing a simulation platform for both Power system and communication network is given in [14], importantly authors have given a flowchart to select a particular platform, based on the type of Simulation, for example, RT or off-line simulation, time domain analysis of the power system or just event-driven etc..

A distributed infrastructure of network systems to communicate with the RT digital simulator allowing the Co-simulation for smart grid application is proposed in [19], also, use of model-based design has been recommended in this work. A Co-simulation platform for distributed grid voltage control using real-time simulator (RTS) for power system component simulation and event-driven systems connected over TCP/IP is proposed in [13], MATLAB environment is used for control action to co-simulate with other system components running in RTS. IEC 61850 protocol to transfer Generic Object Oriented Substation Events (GOOSE) messages over the network using RTS is proposed in [20], more emphasis is given on industrial standard communication, allowing to keep hard real-time properties over the network during simulation.

The power system simulator is time step driven, whereas, the network simulators are event-driven. There should be coherence in execution with the distributed simulators, to execute the simulation, the works [14], [21], [22] briefs about
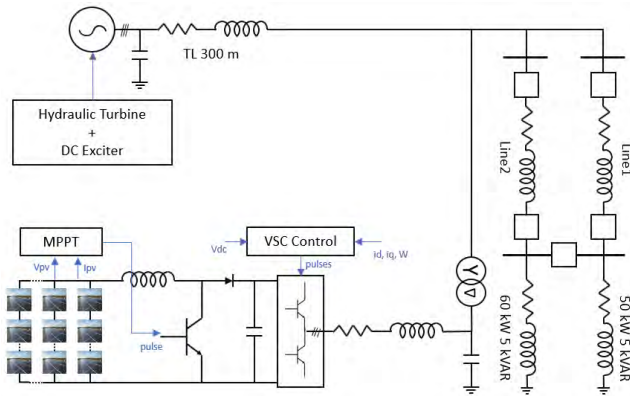
**FIGURE 1.** Microgrid model used in RT simulation.

**TABLE 1.** PV-UD180MF5 PV Module details and parameters for 100 kW array.

| Symbol | Parameter | Value |
|--------|-----------|-------|
| $V_{oc}$ | Open circuit voltage | 30.4 V |
| $I_{sc}$ | Short circuit current | 8.03 A |
| $P_{max}$ | Maximum power rating | 180 W |
| $V_{max}$ | Voltage @ maximum power | 24.2 V |
| $I_{max}$ | Current @ maximum power | 7.45 A |
| $N_{cell}$ | Number of series connected cells in module | 50 |
| n | Diode ideal factor | 1.7 |
| $E_g$ | Band Energy Gap | 1.121 eV |
| $k_i$ | $I_{sc}$ temperature Co-efficient | 0.0032 $K^{-1}$ |
| $R_{sh}$ | Shunt resistance | 3.767 $\Omega$ |
| $R_s$ | Series resistance | 0.00019 $\Omega$ |
| $N_s$ | Number of series modules used | 11 |
| $N_p$ | Number of Parallel Strings used | 51 |

synchronizing methods that can be employed in smart grid Co-simulation. A distributed modeling and Co-simulation platform for European electrical system studies, geographically separated but networked over cloud for advanced European research are reported in the work [23]. A test-bed for real-time simulation of the smart grid is employed in [24], but the communication model is not addressed. HIL simulation to test TU's is proposed in [25], but to generate the fault current LABVIEW software package is used which can potentially increase the development time and also complex smart grid system may require strenuous efforts to realize. The main advantages of the proposed platform over other RTS are, the ability to integrate custom devices and the other simulators for Co-simulation, easily expandable IO nodes according to the grid needs for the simulation, modeling in an independent platform allowing to address a wide variety of the simulation needs and finally, it is cost-effective and modular in nature.

## III. SMART MICROGRID AND ITS COMPONENTS

In order to validate the methodology, proper presentation of the system is a must, and it starts from a real case of the network to simulate, describing its implementation in steps clarifies the methodology we want to propose. In this section we will describe the main components of the network and its general architecture, including the equations we want to implement.

The smart microgrid consists of AC and DC system, A 100 kW Photovoltaic (PV) array with maximum power point tracking control and a boost converter makes the DC system of the microgrid, whereas, the AC system is powered by 250 kVA/400 V synchronous machine connected to a hydraulic turbine and exciter. Other components present in the microgrid are a transformer, transmission lines, voltage source converter for DC to AC conversion of power, Circuit breakers, loads, respective controllers for voltage, current and frequency regulation and finally the communication network between breakers for coordination. Connection diagram of the smart microgrid is as shown in Figure1.

### A. PV ARRAY MODEL

A 100 kW PV array is modeled using the equations as mentioned in [26], PV equation by considering a diode in parallel with current source including series and shunt resistance is given by Equation1,

$$I_{ph} - I_0[e^{(\frac{V_d}{V_t})} - 1] - \frac{V_{pv}}{R_{sh}} - I_{pv} = 0 \qquad (1)$$

where,

| | |
|---|---|
| $I_{pv}$ | cell current |
| $I_{ph}$ | photo current |
| $I_{sh}$ | Shunt current |
| $I_o$ | Diode saturation current |
| $R_{sh}$ | PV shunt resistance |
| $V_d, V_t$ | Diode terminal and thermal voltage |

The Equation1 is solved using Newton Raphson method for $I_{pv}$ or $V_{pv}$ according to the requirement. In this work, a current delivery model is in use, hence the voltage across PV terminal $V_{pv}$ is given while solving to obtain $I_{pv}$. 180 W Mitsubishi Electric PV-UD180MF5 PV Module data is used to model PV array, its parameters are given in Table1. An MPPT controller and a boost converter are used to extract the maximum power from PV. MPPT controller [27] decides the duty cycle D to match the output resistance to be the maximum power extracting point of IV curve of PV characteristics.

### B. SYNCHRONOUS MACHINE AND HYDRAULIC TURBINE

The AC system is modeled using MATLAB Simulink tool using its built-in power system library, 250 kVA/400 V salient pole synchronous machine defined by $6^{th}$ order state space model [28] is used in this work and its parameters are given in Table2. The synchronous generator is coupled to a hydraulic turbine which is regulated using a PID control system which serves according to the needs of the grid for power delivery and to run in synchronous speed to maintain the grid frequency.

### C. EXCITATION SYSTEM

The excitation system of IEEE standards type1 is used [29], the dynamics of the exciter is given by Equations 2,3,4, and

**TABLE 2. Synchronous generator parameters.**

| Symbol | Parameter | Value |
|---|---|---|
| w | Frequency | 50 Hz |
| $x_d, x_d', x_d''$ | Direct axis reactances | 1.5 pu, 0.3 pu, 0.4 pu |
| $x_q, x_q', x_q''$ | quadrature axis reactances | 1.1 pu, 0.7 pu, 0.5 pu |
| H | Inertia constant | 0.1753 s |
| F | Friction factor | 0.01579 pu |
| P | Number of pole pairs | 2 |

**TABLE 3. Turbine and exciter parameters.**

| Symbol | Parameters | Value |
|---|---|---|
| $k_a$ | Servo motor gain | 3.33 |
| $T_a$ | Servo motor time constant | 0.07 s |
| $g_{min}$ and $g_{max}$ | Gate opening limits | 0.01 pu, 0.91578 pu |
| $vg_{min}$ and $vg_{max}$ | Limits of gate speed | -1 pu/s and 1 pu/s |
| $R_p$ | Static gain | 0 |
| $k_p, k_i, k_d$ | PID gains | 0.8, 0.305,0 |
| $T_d$ | Low pass filter time constant | 0.01s |
| $\beta$ | damping co-efficient | 0 |
| $T_w$ | water starting time | 0.267s |
| $k_r, k_e, k_f$ | Exciter gains | 10, 1, 0.001 |
| $T_r, T_e, T_f$ | Exciter time constants | 1 s, 1 s, 0.1 s |
| $E_{fmin}, E_{fmax}$ | regulator output limits | 0 pu, 2 pu |

the relevant parameters are given in Table3.

$$T_E \frac{dE_{fd}}{dt} = V_R - \left(K_E + S_E(E_{fd})\right) E_{fd} \tag{2}$$

$$T_A \frac{dV_R}{dt} = -V_R + K_A R_F - \frac{K_A K_F}{T_F} E_{fd} + K_A (V_{ref} - V_t) \tag{3}$$

$$\frac{dR_F}{dt} = -R_F + \frac{K_F}{T_F} E_{fd} \tag{4}$$

where,

| | |
|---|---|
| $K_E$ | Gain of the DC exciter |
| $T_E$ | Time constant of the DC exciter |
| $E_{fd}$ | DC generator output armature voltage |
| $K_A$ | Gain of the Voltage regulator |
| $T_A$ | Time constant of the voltage regulator |
| $V_t$ | voltage of transducer of load compensator |
| $V_R$ | voltage regulator output for error $v_{in}$ |
| $S_E(E_{fd})$ | Saturation function |
| $K_F$ | stabilizing transformer gain |
| $R_F$ | Rate feedback of stabilizing transformer |
| $T_F$ | Time constant of the stabilizing system |

### D. VSC CONVERTER AND ITS CONTROL

VSC converter is used to bridge the DC and AC system, the power generated from PV will be pushed to the grid using a 3 arm IGBT converter. VSC controller has the ability to provide ancillary support to the synchronous generator by generating or by absorbing reactive power with the switching control of the converter. It has an inner current control loop and outer voltage and frequency control loop. By measuring the frequency, demanded $i_q^*$ reference is given to the controller for better frequency regulation as mentioned in [30], [31]. The VSC controller schematic diagram is given in the Figure 2, three phase voltage $V_{abc}$ at PCC is measured and split into its constituents $V_d$ and $V_q$, the DC bus voltage measured $V_{dc}$ and the grid frequency w is given as inputs to the controller
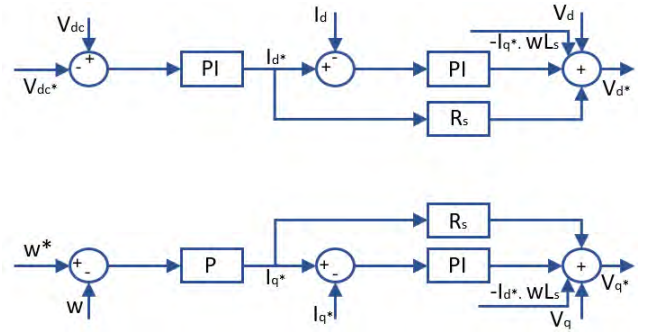


**FIGURE 2. VSC control with outer Voltage and frequency control and inner current control loop.**

and the output $V_d^*$ and $V_q^*$ from the controller is used to obtain the pulses for VSC converter by adopting appropriate transformations.

### E. REST OF THE COMPONENTS

The AC and DC system meets at the point of common coupling (PCC) in the microgrid. The converter output is given to RLC filter then connected to PCC using $3\phi$ transformer, whereas, the generator is connected to PCC via a 300m transmission line. Two transmission lines are tapped onto PCC, and they have circuit breakers at both the ends. The ends are connected to the bus where the loads are tapped for power consumption, 50 kW 5 kvar load is connected to line1 whereas, 60 kW 5 kvar load is connected to line2. The load buses are also connected as shown in the Figure 1, using a Circuit breaker for uninterrupted power supply.

### IV. HIL SIMULATION FRAMEWORK

The main intention of this work is to reduce the modeling time of the electrical system for real-time simulation, allowing to store and reuse models made in other simulation environments. Moreover the proposed system wants to be modular and implementable in hardwares typologies easily available, as well as intel based computers, without necessarily having to use dedicated systems. With the use of automatic code generating tool, it is possible to use the inbuilt power system library and to generate C-code enabling to run in the Intel processor of the PC externally out of Simulink using a software add on called Simulink desktop real-time (SLDRT)(will be called as platform 1) kernel. The C-code generated out of the model also includes a solver definition and the parameters library, which helps to keep the original behavior of the modeled system.

The choice of the simulator is completely arbitrary and can also be made starting from direct models written in C or other simulation environments that allow the generation of the code.

To this is real-time simulation platform, we need additional customization to conduct HIL simulation, and it is done by implementing a Co-simulation architecture with the incorporation of another real-time digital simulator having generic hardware integration capability. In this work c-RIO
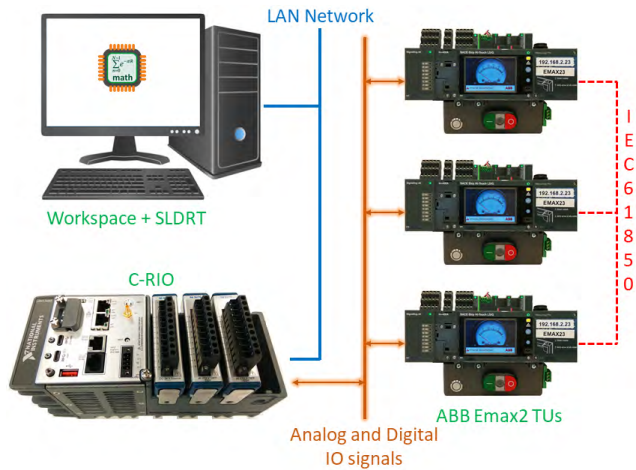
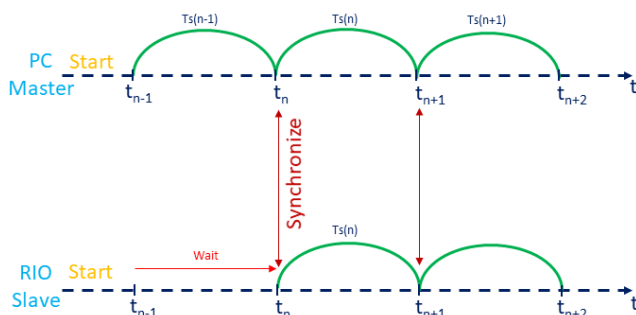**FIGURE 3.** RTS integration with the TUs and the communication network.



**FIGURE 4.** Master and slave time synchronization between the RTS.

running LABVIEW RTOS (will be called as platform 2) is used as the digital simulator that co-simulates with platform 1 to execute the real-time simulation of the smart grid, model is split into two sections and simulated in real-time using HIL methodology, one of the section is emulated in Intel processor of desktop PC while the other section is emulated in the c-RIO and these simulators are connected over Ethernet network. The models running in real-time are interfaced using UDP protocol over Ethernet to exchange the voltage and current data in run-time by implementing the Master-slave time synchronization method. platform 1 is master, and it synchronizes with platform 2 for data exchange. meanwhile, platform 2 waits till it receives the command from the platform as shown in the Figure 4. This enables the user to test the smart grid scenarios, as the network emulation is also considered in this case. Again, the choice of solution is entirely arbitrary, and can be replaced by any system with FPGAs.

Another way to implement the smart grid scenario is to use the physical hardware devices that are interconnected using standard industrial communication protocols such as IEC 61850. As the proposed platform in this work is a Co-simulation environment, Platform 1 has well-built power system library, and c-RIO comes with a powerful processor and FPGA for signal generation and acquisition, hence using this setup full smart grid model can be tested in real-time. Most of the communication network involved in smart grid is used by
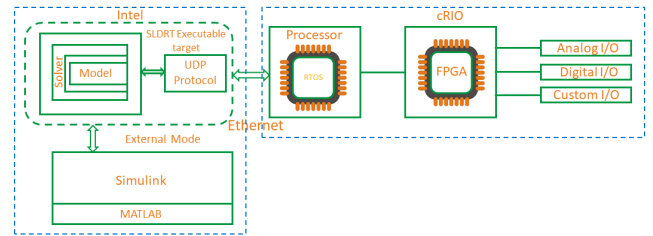
**FIGURE 5.** Co-simulation architecture used for RT simulation of Smartgrid.

its protection devices for coordination, selectivity, and control in case of load shedding. This proposed platform provides a wonderful opportunity to include these protection devices in the simulation. The circuit breakers will have an electronic control unit called a trip unit, it measures the current and voltage of the line, in turn, acts according to the set logic when the event occurs.

Current and voltage signals generated by the simulation system are given to the trip units, and status signals are used to close the loop. This enables to test different fault scenarios, grid control and protection scenarios of the smart grid along with the incorporation of time delays encountered in network communication and also the theoretical consideration of the breaker opening time is eliminated by real behavior implementation. Proposed connection between the real-time digital simulators and the trip units using IEC 61850 protocol is shown in the Figure3.

### A. HIL CO-SIMULATION ARCHITECTURE
Two RTS are connected over the network in their root functionality level as shown in the Figure5, platform 1 runs a real-time kernel operating system in the processor using the basic CPU clock as the timing source. This functionality allows the user to reach smaller time steps up to $5\mu s$ theoretically, 200 kHz signal can be simulated [17] by running the model externally out of Simulink and running directly in the processor of the general PC having the clock speed of 2.25 GHz. This small time step of $5\mu s$ is small enough to capture the electromagnetic transients that can appear in the smart grid. The kernel OS running in processor contains a checksum number, which checks the match between loaded executable C-code and original model. Another important characteristic of the kernel is, it loads the executable C-code and conserves the clock sequence to keep hard real-time properties.

The platform2 in cRIO runs with reconfigurable IO architecture, which has a real-time processor and a reconfigurable FPGA [18]. Intel Atom dual-core processor at 1.33 GHz is used, in which platform can simulate up to 40 MHz while keeping hard real-time properties using a user-defined model, measurement IO modules help to drive signals from machine to the real world and vice versa. the processor runs RT operating system, and loads the user-designed virtual instrument defining the model functions and also manages the network adapters required for network communication and capable of communicating up to the speed of 1000 Mbps. FPGA runs the predefined configuration file called bit file, which is obtained
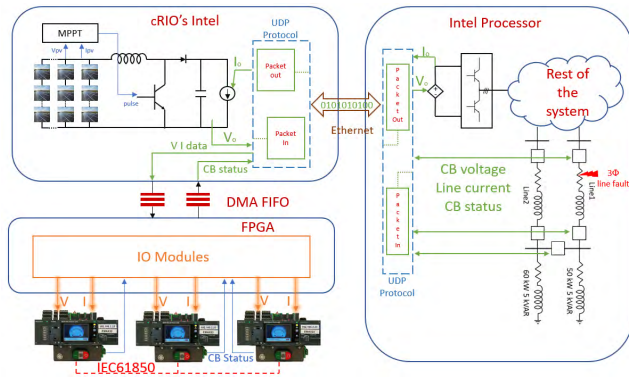
**FIGURE 6.** Smartgrid real-time simulation setup along with the physical breaker and emulated PV system in the loop.



**FIGURE 7.** An analogy of how trip unit realizes simulated signal as real measured current.

after configuring the FPGA usage and compiling it using appropriate compiling tool. Data transfer between processor and FPGA is done using First-in First-out (FIFO) direct memory access (DMA) buffers. UDP protocol is used to connect the two systems over Ethernet, out of much available communication protocol, this method is used by considering the communication speed which is needed to keep the hard real-time properties. The RT targets are considered as nodes, and as many nodes can be considered until they are in the same network.

## V. TESTBENCH SETUP OF RT SIMULATION

The test setup of Smartgrid RT simulation is given in Figure 6, DC system of the smart grid is considered in HIL loop along with physical breakers. A controlled current source is used to close the loop of the boost converter, the output voltage of the converter is measured and bundled as data packets which are sent over Ethernet to power the controlled voltage source of the VSC converter.

The ideal circuit breakers that interrupt the current at zero crossings with the trip signal is modeled using model based designing tool, breaker voltage in the smart grid system and line current flowing through the breaker are bundled and sent to cRIO using UDP over the network, cRIO reads the data packet and sends this data to FPGA using DMA FIFO buffers to regenerate real-time signal. In the same way, CB status of the physical breaker is sent from cRIO to the simulated breakers in platform 1 as a trip command to interrupt the current flow. Digital input module is used to interface the TU and FPGA.

Using Analog output module, signals are driven out of simulation and applied on the breaker. The TU's are programmed to measure the real current and voltage using respective sensors, the voltage measurement is bypassed, with appropriate scaling. The TUs determines the current using Rogowski coils. TU measures the voltage across the Rogowski coil, as the inductance of the coil is known, the current will be deduced using the relation as given in Equation 5.

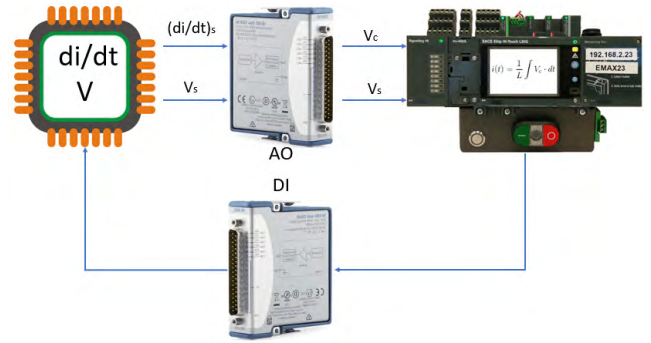$$i(t) = \frac{1}{L} \int V_c \cdot dt \qquad (5)$$

where,

$i_t$     Current measured

$L$     Rogowski coil inductance

$V_c$     Voltage measured across the Rogowski coil

Signals generated by the simulation systems must match with the above processing, so that the trip unit measures the correct value of the simulated current. To this purpose, a voltage signal proportional to current derivative is generated. Scaling to ± 10V is also applied to avoid channel saturation. The analog output module will generate the voltage signal which is applied on the trip unit measurement terminals as shown in Figure7.

## VI. SIMULATION AND RESULTS

A 100 kW PV mathematical model and other DC system is emulated in hardware of platform 2 using script block, at 25°C, 1000 W/$m^2$ of temperature and irradiance input, it will deliver 100 kW of power to the VSC converter running in another simulator. A three-phase line fault is considered in this experiment, to test the coordination between the breakers and to study the microgrid behavior in response to the fault clearance by the breaker to provide uninterrupted supply.

Consider the breakers CB1, CB2, CB3, CB4 and CB5 positioned as shown in Figure8, in this work CB1, CB2 and CB3 are connected using IEC-61850 industrial standard communication protocol. CB1 and CB2 are connected with interlock/intertrip and protection GOOSE while CB2 and CB3 are sharing only interlock GOOSE messages. Let a three-phase fault act in line1 immediately below CB1.

CB1 and CB2 exchange protection GOOSE messages, informing each other about fault currents they detect. CB2 detects no fault current: based on such information, CB1 decides to trip, because it is the first breaker upstream the fault. CB1 thus trips. In addition, it sends an intertrip message to the next breaker (i.e., CB2) commanding it to open and remove the faulted zone from service. CB2, in turn, after opening, sends command message to CB3, which closes and restores power to the load bus.

After modeling AC systems of the smart grid, a fixed step Euler solver with 0.1 ms time steps are selected, later model is built to generate C-code and run in an external model using
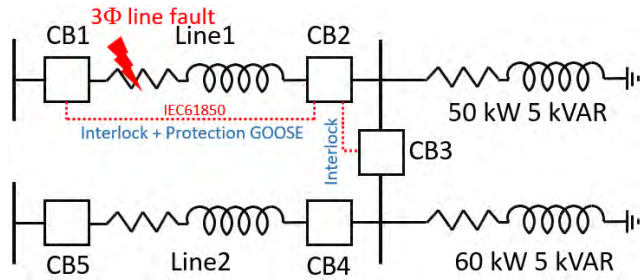
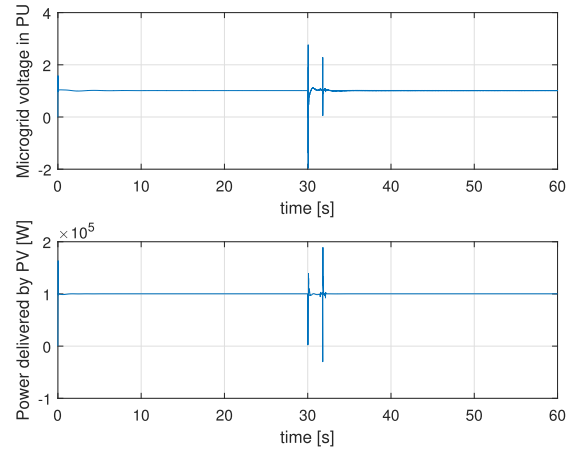**FIGURE 8.** Interlock and protection GOOSE messages between the breakers.
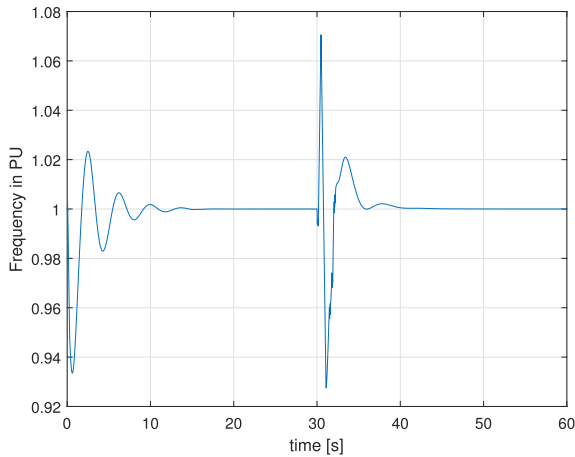


**FIGURE 9.** Microgrid frequency in PU, fault created at 30 S and the starting instants shows the synchronous machine behavior and later it is with frequency control.



**FIGURE 10.** Voltage of the Microgrid in PU and the Power delivered by PV in Watts.



**FIGURE 11.** Three phase current derivative measured using oscilloscope.

Platform 1 kernel. The generation of C code requires a compiler, and specific concerns are taken in selecting or writing the solvers and time steps of the execution. The detailed information regarding the compiler, kernel, and implementation is given in [17]. Also, the main idea of this work is to use the built-in library of the power system simulators, only the model simulated in platform 2 and the PV model running platform 1 is custom and the rest others are the built-in model of simulink library. The sample time of the generated signal can also be interpreted as electromagnetic transient signals up to 10 kHz can be generated and imposed on breakers without aliasing.
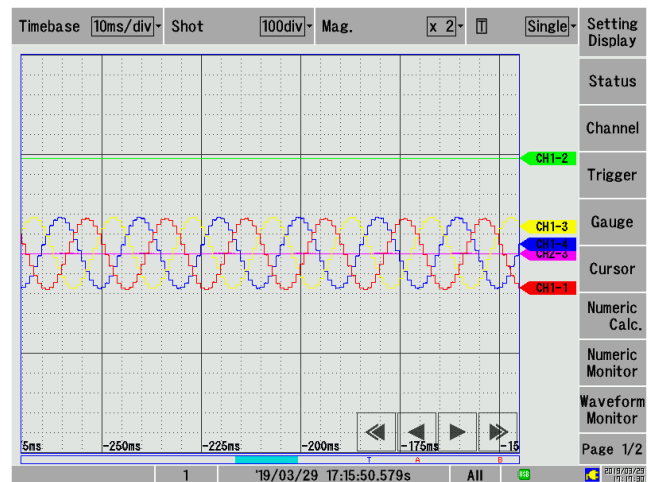
The synchronous machine is allowed to settle on its own without frequency control and later it is turned on. The fault is created at the instant of the 30s, and the microgrid behavior is observed. The variation in the frequency of microgrid in PU due to the fault and co-ordination of breakers in its clearance is given in Figure9.

Frequency control helps in better regulation and operation of the microgrid, and it can be observed by the frequency behavior of the microgrid. VSC controller provides ancillary support to the synchronous machine by varying the switching patterns of the converter.

The power delivered by PV system running synchronously in cRIO and the voltage of PCC in PU is given in Figure10.

The first spike observed is due to the fault whereas, the second spike is due to the aggressive frequency control. The power delivered by PV is 100 KW, as the Irradiation and the temperature are 1000 $W/m^2$ and 25°C respectively, maintained constant throughout the simulation. The Power delivered by PV shows the successful synchronization of the Co-simulation platform.

The current and voltage seen by the breakers in the simulation are applied on TUs with the method described above. The derivative of the current applied on TU corresponding to CB1 as measured using an oscilloscope is shown in Figure11.

The simulated microgrid frequency is set at 50 Hz, the measured signal frequency is indeed 50Hz, showing that the system is able to work in real time.

$3\phi$ line fault is generated immediately down to CB1 at $30^{th}$ second of simulation, the current seen by CB1 and the protection actions taken by CB1 and CB2 to isolate the faulty line is given in Figure12.

Short circuit protection with adjustable delay is set in the TU linked with CB1 to clear the fault current when it reaches 1.5 times the nominal current with the time setting of 50 ms.
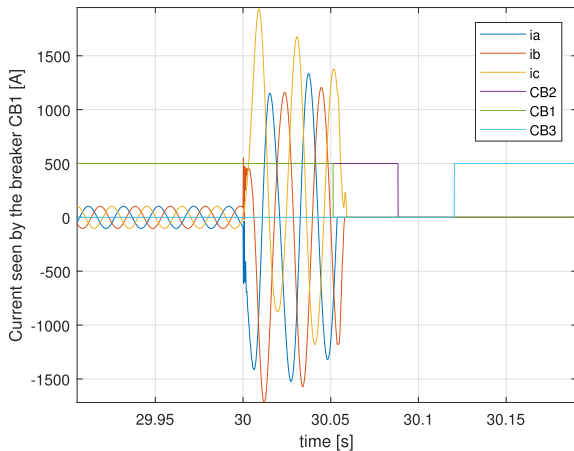
**FIGURE 12.** Fault current seen by CB1 and the CB status of the respective breaker in platform 1.
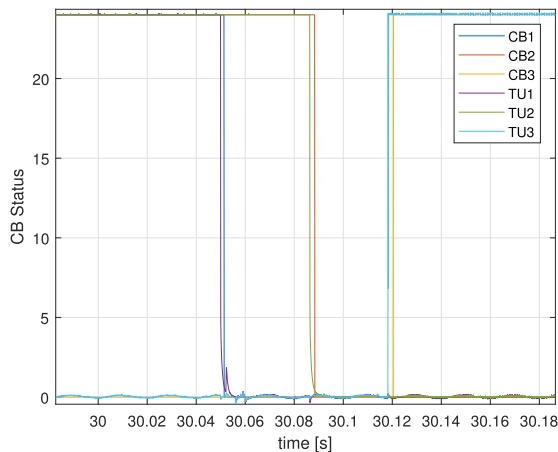


**FIGURE 13.** The status of the trip units as seen by cRIO and the circuit breaker status in the platform1.

TU recognizes the fault current at t = 30s and waits for 50 ms, later it sends the S-trip signal and changes the status of the CB1 to open, the change in status is measured using ADC associated with the FPGA and sent to the simulated CB1 in the platform1. CB1 receives the trip status at 51.4 ms after the fault, and all the three currents reach zero by 59.2 ms after fault. TU1 sends GOOSE message CB open to TU2 asking it to open and isolate the faulty line. CB2 is opened at 88.4 ms after fault occurrence. Later, TU2 sends CB close GOOSE message to TU3 asking it to close and to connect the load bus to the bus connected to line2 which is in service. CB3 will be closed at 120.4 ms after fault occurrence and ensures the supply to the load without a long power gap.

The above-mentioned timings are the timestamps in the real-time simulation executing in platform 1, but actually, there exists a finite delay between the TU coordination in the real world and the signal received in simulation after processing. To measure this delay, the TUs status is measured and logged using an oscilloscope, and later it is compared with the timestamps of real-time simulation.

Figure13 shows the timestamps when the status of the trip units are measured by FPGA of cRIO and the status of the respective simulated circuit breakers related to the trip units. TU1(Physical hardware) and CB1 (Simulated in platform 1) have a delay of 1.4 ms whereas TU2 and CB2, as well as TU3 and CB3, has 2ms of delay between them. Such delays are due to signal transfer between the Co-simulation components, and because they are much less than the typical operation time of switching devices that typically has the trip time of 3 ms, and mechanical operation time of about 40 ms, so devices receive realistic feedback from current and voltage input, these delays are compatible for the testing procedures of the breaker.

One interesting application of our simulation platform is that it allows measurement of delays due to communication and processing in real devices: e.g., in the above case, a time difference of 36.6 ms was measured between tripping of TU1 and TU2, and a difference of 31.7ms between tripping of TU2 and closing of breaker by TU3. These delays are due to internal workings of the devices, and we can expect to find a similar behavior on field. Based on these results, it is then possible to assess if a given set of devices, connected in a specific way, will be able to respond to a fault within the specified time.

## VII. CONCLUSION

The need for cost-effective and quick modeling solution for testing and simulation of the smart grid including the communication network behavior also with the physical hardware integration is well addressed in this work. The proposed test bench can be used to study smart grid control design and to check its behavior with a wide variety of hardware integration. At first, the HIL approach of simulating the PV system behavior successfully demonstrates the ability of the platform to conduct Co-simulation with the physical network emulation with a virtual system. Later the HIL setup successfully demonstrated the ability to integrate the physical hardware trip units for testing control and coordination. The time delay encountered in bridging the real-world with the simulated system is about 2ms, it shows an acceptable performance of the proposed platform for Smart grid real-time simulation and hardware integration tests.

## REFERENCES
[1] Y. Ding, S. Pineda, P. Nyeng, J. Østergaard, E. M. Larsen, and Q. Wu, "Real-time market concept architecture for EcoGrid EU—A prototype for European smart grids," *IEEE Trans. Smart Grid*, vol. 4, no. 4, pp. 2006–2016, Dec. 2013.

[2] C. Shum, W. H. Lau, K. L. Lam, Y. He, H. Chung, N. C. F. Tse, K. F. Tsang, and L. L. Lai, "The development of a smart grid co-simulation platform and case study on vehicle-to-grid voltage support application," in *Proc. IEEE Int. Conf. Smart Grid Commun. (SmartGridComm)*, Oct. 2013, pp. 594–599.

[3] P. Zhang, F. Li, and N. Bhatt, "Next-generation monitoring, analysis, and control for the future smart control center," *IEEE Trans. Smart Grid*, vol. 1, no. 2, pp. 186–192, Sep. 2010.

[4] H. Palahalli, Y. Huo, and G. Gruosso, "Real time simulation of photovoltaic system using FPGA," in *Proc. IEEE Int. Symp. Power Electron., Elect. Drives, Autom. Motion (SPEEDAM)*, Jun. 2018, pp. 865–870.

[5] M. D. O. Faruque, T. Strasser, G. Lauss, V. Jalili-Marandi, P. Forsyth, C. Dufour, V. Dinavahi, A. Monti, P. Kotsampopoulos, J. A. Martinez, K. Strunz, M. Saeedifard, X. Wang, D. Shearer, and M. Paolone, "Real-time simulation technologies for power systems design, testing, and analysis," *IEEE Power Energy Technol. Syst. J.*, vol. 2, no. 2, pp. 63–73, Jun. 2015.

[6] V. R. Dinavahi, M. R. Iravani, and R. Bonert, "Real-time digital simulation of power electronic apparatus interfaced with digital controllers," *IEEE Trans. Power Del.*, vol. 16, no. 4, pp. 775–781, Oct. 2001.

[7] H. K. Fathy, Z. S. Filipi, J. Hagena, and J. L. Stein, "Review of hardware-in-the-loop simulation and its prospects in the automotive area," *Proc. SPIE*, vol. 6228, May 2006, Art. no. 62280E.

[8] J. Leitner, "A hardware-in-the-loop testbed for spacecraft formation flying applications," in *Proc. IEEE Aerosp. Conf.*, vol. 2, Mar. 2001, pp. 2–615.

[9] S. C. Oh, "Evaluation of motor characteristics for hybrid electric vehicles using the hardware-in-the-loop concept," *IEEE Trans. Veh. Technol.*, vol. 54, no. 3, pp. 817–824, May 2005.

[10] C. S. Edrington, M. Steurer, J. Langston, T. E. Mezyani, and K. Schoder, "Characteristics and design of power hardware-in-the-loop simulations for electrical power systems," *IEEE Trans. Ind. Electron.*, vol. 63, no. 1, pp. 406–417, Jan. 2016.

[11] X. Guillaud, A. Faruque, A. Teninge, A. H. Hariri, L. Vanfretti, M. Paolone, V. Dinavahi, P. Mitra, G. Lauss, C. Dufour, P. Forsyth, A. K. Srivastava, K. Strunz, T. Strasser, and A. Davoudi, "Applications of real-time simulation technologies in power and energy systems," *IEEE Power Energy Technol. Syst. J.*, vol. 2, no. 3, pp. 103–115, Sep. 2015.

[12] J.-N. Paquin, W. Li, J. Bélanger, L. Schoen, I. Peres, C. Olariu, and H. Kohmann, "A modern and open real-time digital simulator of all-electric ships with a multi-platform co-simulation approach," in *Proc. IEEE Electr. Ship Technol. Symp. (ESTS)*, Apr. 2009, pp. 28–35.

[13] J. Krata, "A real-time co-simulation platform for distribution grid voltage control," in *Proc. IEEE Australas. Universities Power Eng. Conf. (AUPEC)*, Nov. 2017, pp. 1–6.

[14] W. Li, M. Ferdowsi, M. Stevic, A. Monti, and F. Ponci, "Cosimulation for smart grid communications," *IEEE Trans. Ind. Informat.*, vol. 10, no. 4, pp. 2374–2384, Nov. 2014.

[15] T. Godfrey, S. Mullen, D. W. Griffith, N. Golmie, R. C. Dugan, and C. Rodine, "Modeling smart grid applications with co-simulation," in *Proc. 1st IEEE Int. Conf. Smart Grid Commun. (SmartGridComm)*, Oct. 2010, pp. 291–296.

[16] P. Palensky, E. Widl, M. Stifter, and A. Elsheikh, "Modeling intelligent energy systems: Co-simulation platform for validating flexible-demand EV charging management," *IEEE Trans. Smart Grid*, vol. 4, no. 4, pp. 1939–1947, Dec. 2013.

[17] *Simulink Desktop Real-Time User Manual*. Accessed: 2018. [Online]. Available: https://www.mathworks.com/

[18] *National Instruments cRIO-9031 User Manual*. Accessed: 2018. [Online]. Available: http://www.ni.com/

[19] L. Bottaccioli, A. Estebsari, E. Pons, E. Bompard, E. Macii, E. Patti, and A. Acquaviva, "A flexible distributed infrastructure for real-time cosimulations in smart grids," *IEEE Trans Ind. Informat.*, vol. 13, no. 6, pp. 3265–3274, Dec. 2017.

[20] M. Manbachi, A. Sadu, H. Farhangi, A. Monti, A. Palizban, F. Ponci, and S. Arzanpour, "Real-time co-simulation platform for smart grid volt-VAR optimization using IEC 61850," *IEEE Trans. Ind. Informat.*, vol. 12, no. 4, pp. 1392–1402, Aug. 2016.

[21] H. Lin, S. S. Veda, S. S. Shukla, L. Mili, and J. Thorp, "GECO: Global event-driven co-simulation framework for interconnected power system and communication network," *IEEE Trans. Smart Grid*, vol. 3, no. 3, pp. 1444–1456, Sep. 2012.

[22] C.-H. Yang, G. Zhabelova, C.-W. Yang, and V. Vyatkin, "Cosimulation environment for event-driven distributed controls of smart grid," *IEEE Trans. Ind. Informat.*, vol. 9, no. 3, pp. 1423–1435, Aug. 2013.

[23] C. F. Covrig, G. De Santi, G. Fulli, M. Masera, M. Olariaga, E. Bompard, G. Chicco, A. Estebsari, T. Huang, E. Pons, and F. Profumo, "A European platform for distributed real time modelling & simulation of emerging electricity systems," Publications Office Eur. Union, Brussels, Belgium, JRC Rep. JRC101772, EUR 27941, 2016.

[24] P. Tatcho, Y. Zhou, H. Li, and L. Liu, "A real time digital test bed for a smart grid using RTDS," in *Proc. IEEE 2nd Int. Symp. Power Electron. Distrib. Gener. Syst.*, Jun. 2010, pp. 658–661.

[25] L. Bertoletti, E. Ragaini, and J. Liu, "Hardware-in-the-loop simulation for testing low voltage circuit breakers selectivity," in *Proc. IEEE Int. Conf. Environ. Elect. Eng., IEEE Ind. Commercial Power Syst. Eur. (EEEIC/I CPS Eur.)*, Jun. 2017, pp. 1–5.

[26] H.-L. Tsai, C.-S. Tu, and Y.-J. Su, "Development of generalized photovoltaic model using MATLAB/SIMULINK," in *Proc. World Congr. Eng. Comput. Sci.*, San Francisco, CA, USA, 2008, pp. 1–6.

[27] B. Subudhi and R. Pradhan, "A comparative study on maximum power point tracking techniques for photovoltaic power systems," *IEEE Trans. Sustain. Energy*, vol. 4, no. 1, pp. 89–98, Jan. 2013.

[28] P. C. Krause, *Analysis of Electric Machinery and Drive Systems*. New York, NY, USA: McGraw-Hill, 1986.

[29] D. Lee, *IEEE Recommended Practice for Excitation System Models for Power System Stability Studies*, IEEE Standard 421.5-2016, Energy Development and Power Generating Committee of the Power Engineering Society, vol. 95, no. 96, 1992.

[30] Y. Huo, S. Barcellona, G. Gruosso, and L. Piegari, "Definition and analysis of an innovative ancillary service for microgrid stability improvement," in *Proc. IEEE Int. Symp. Power Electron., Elect. Drives, Autom. Motion (SPEEDAM)*, Jun. 2018, pp. 990–995.

[31] Y. Huo and G. Gruosso, "Hardware-in-the-loop framework for validation of ancillary service in microgrids: Feasibility, problems and improvement," *IEEE Access*, vol. 7, pp. 58104–58112, 2019.

**HARSHAVARDHAN PALAHALLI** (M'19) was born in 1992. He received the bachelor's degree in electrical and electronics engineering from Visvesvaraya Technological University, India, in 2014, and the master's degree in electrical engineering from Politecnico Di Milano, Italy, in 2018. He is currently with the ABB as a Graduate Intern. His research interests include real-time simulation of electric systems, including design, and modeling renewable energy systems.

**ENRICO RAGAINI** graduated in electronics engineering and received the Ph.D. degree in electrical engineering from Politecnico di Milano, in 1991 and 1996. After serving 2 years as a Professor with Universidad de Piura, Peru, he joined ABB, first in Corporate Research and then in the Low Voltage Products division. He held various positions including Product Manager for Low Voltage Circuit Breakers, focusing on electronic protection units, embedded communication, and system supervision. He has then been in charge of Technical Training for the ABB Low Voltage Breakers global factory, from 2004 to 2010, and then as a Cyber Security manager for the ABB Low Voltage Products division, from 2011 to 2014. He is currently with the Research and Development of ABB Low Voltage Circuit Breakers and Switches business unit, in charge of Systems and Applications.

He is also a Professor of Electrical Switching Devices at Politecnico di Milano. His research interests include electrical measurements, protection and switching devices, and real-time simulation of power systems.

**GIAMBATTISTA GRUOSSO** (M'01–SM'12) was born in 1973. He received the M.S. degree in electrical engineering from the Politecnico di Torino, Italy, in 1999 and the Ph.D. degree in electrical engineer from Politecnico di Torino, Italy, in 2003. From 2002 to 2011, he was an Assistant Professor with the Department of Electronics and Informatics, Politecnico di Milano. Since 2011, he has been an Associate Professor with Politecnico di Milano. He does research in electrical engineering, electronic engineering and industrial engineering. His main research interests include electrical vehicles transportation electrification electrical power systems optimization, and simulation of electrical systems. He is the author of more than 100 papers on journals and conferences on the topic.

. . .